SLAC-CN--372

DE90 003763

SINGLE PASS COLLIDER MEMO CN-372

AUTHOR: C. Fordham DATE: November 2, 1989

TITLE: THE RELATION OF ELECTRODE VOLTAGES TO CHARGE POSITION IN SLC ARC AND FINAL FOCUS BEAM POSITION MONITORS*

1. INTRODUCTION

The position of a charged particle beam can be measured with a Beam Position Monitor (BPM) by converting the voltages induced on its array of electrodes into a position offset from the array's center. Most of the BPMs in the Arcs and Final Focus of the SLC use four stripline electrodes arranged symmetrically around the beam; normalized voltage differences are calculated as the difference divided by the sum of voltages on opposite electrode pairs. The resulting number is multiplied by a conversion factor, denoted in this paper as S_b, to give the offset (in millimeters) of the charge from the center of the BPM.

Prior to installation in the beam line, the BPMs were calibrated with a charge pulse on a rod. Owing to geometric effects which will be discussed later, a different conversion factor had to be used for calibration. It will be denoted here by S_r.

This paper gives the results of calculations and measurements of S_r and S_b for Arc and Final Focus BPMs. Section 2 describes the relevant physical properties of the several types of BPMs and calculations of the expected scale factors, Section 3 describes the measurement methods used, and Section 4 gives the results of measurements, which are compared with the theoretical expectations in Section 5.

*Work Supported by the Department of Energy Contract DE-AC03-76SF00515.

2. EXPECTED RESPONSE OF BPMS

2.1. Structure of the Arc and Final Focus BPMs

The BPMs in the Arc and Final Focus regions of the SLC consist of four striplines in a vacuum pipe. The striplines run parallel to the beam and are evenly spaced around it with their centers at 45° to the beam coordinate system. They are grounded at one end, with signal feedthroughs penetrating the vacuum pipe at the other end. The striplines subtend 45° of arc in ϕ and are separated from the vacuum pipe at a distance that will give 50 Ω impedance. Fig. 1 shows the structure of the Arc-type BPM and Fig. 2 that of the standard Final Focus BPM. Table 1 lists the BPM cross-section dimensions.

Table 1: Dimensions of BPMs

Type	Electrode Inner Radius	Electrode Outer Radius	Vacuum Pipe Inner Radius
Arc	7.25 mm	8.33 mm	10.33 mm
Final Focus 1″	9.68 mm	10.96 mm	12.79 mm
Final Focus 2″	19.23 mm	21.77 mm	25.4 mm
Final Focus 5″	48.08 mm	54.43 mm	63.4 mm

The Final Focus BPM comes in three sizes, 1″, 2″, and 5″ diameter. They were designed to have the same length electrodes and cross sections identical except for the radial scaling, so their electrical properties are the same except for a scaling of S linearly with the radius. The calculations and measurements in this paper for the Final Focus BPMs were done for the 2″ diameter size for reasons of convenience; that size best fits the measurement apparatus.

2.2. CALCULATION OF S_b

Displacement of charges in a BPM with four electrodes at zero degrees to the beam coordinates are calculated as follows:

$$x = S_b \frac{(V_1 - V_3)}{V_1 + V_3} \tag{2.1}$$

$$y = S_b \frac{(V_2 - V_4)}{V_2 + V_4} \tag{2.2}$$

Note that S_b for the x calculation and the y calculation is assumed to be the same, which should be the case for a $\frac{\pi}{2}$ rotationally symmetric BPM.

For beam measurement at the SLC, S_b is assumed to be constant. This is a reasonable approximation for the region near the BPM's center, where most measurements are made. However, the relation between charge positions and normalized voltage differences in BPMs is not actually linear, so the most general S_b is a function of charge displacement rather than a constant. In this paper, S will be calculated as a function for two idealizations of the BPM geometry, and then the limit of zero displacement will be used to give the "constant" S_b.

The BPM will be regarded as an unbroken cylinder; the effects of electrodes protruding into the beam pipe and the effects of the changing size of the beam pipe will be ignored, as will terms coming from a non-cylindrical beam shape. These are treated elsewhere.

Carman and Pellegrin[1] calculated S_b for a line of charge in an idealized SPEAR storage ring BPM. They assume a perfectly cylindrical structure with electrodes small enough so that the field is constant over the surface of the electrode. The image charge for a line charge displaced at polar coordinates (δ, θ) from the axis of a conducting cylinder of radius R is a parallel line of opposite charge at $(\frac{R^2}{\delta}, \theta)$ (Fig. 3). Therefore, the charge distribution on the inside of a conducting cylinder (the BPM) from a line charge displaced at polar coordinates (δ, θ) from the center is

$$q = \frac{a}{2\pi R} F(\delta, \theta, \phi)\, \lambda \tag{2.3}$$

$$F(\delta, \theta, \phi) = \frac{R^2 - \delta^2}{R^2 + \delta^2 - 2R\delta\cos(\phi - \theta)} \tag{2.4}$$

where λ is the charge density of the beam, R the radius of the BPM, a is the electrode area, and ϕ the angular coordinate at the BPM wall. $F(\delta, \theta, \phi)$ contains

the displacement dependent terms. If the electrical properties of all electrodes are identical, $F(\delta,\theta,\phi)$ is the only factor which varies with ϕ and therefore with electrode,so $F(\delta,\theta,\phi)$ can be substituted for V in the position equations. To calculate S_b for non-rotated electrodes, displace the line of charge a distance δ in direction θ. ($\theta = 0$ is defined towards electrode 1.) We can find the value of S_b such that x, the displacement of the charge, can be found with (2.1).

$$x = \delta\cos\theta = S_b\,\frac{F(\delta,\theta,0) - F(\delta,\theta,\pi)}{F(\delta,\theta,0) + F(\delta,\theta,\pi)} \tag{2.5}$$

A little algebra gives

$$S_b = \frac{R^2+\delta^2}{2R} \tag{2.6}$$

which goes to $S_b = \frac{R}{2}$ for small displacements.[1]

2.3. Effects of Electrode Width

This calculation is somewhat too simple for the Arc and Final Focus BPMs; the conducting surfaces near the beam are not an unbroken cylinder, but a superposition of parts of two cylinders of different radii. However, for displacements of the line of charge which are small compared to any of the radii, the field distribution will be similar to that for an unbroken cylinder. Another inadequacy in the previous calculations is the assumption that the field is equal over the whole width of the electrode, which is not valid for broad electrodes, as in the BPMs under study. Correction for this effect demands integration of the field over the surface of the electrode in order to calculate the voltages. Once again all terms except $F(\delta,\theta,\phi)$ cancel out.

$$x = \delta\cos\theta = S_b\,\frac{\int_{-\Delta\phi}^{\Delta\phi} F(\delta,\theta,\phi)d\phi - \int_{-\Delta\phi}^{\Delta\phi} F(\delta,\theta,\phi+\pi)d\phi}{\int_{-\Delta\phi}^{\Delta\phi} F(\delta,\theta,\phi)d\phi + \int_{-\Delta\phi}^{\Delta\phi} F(\delta,\theta,\phi+\pi)d\phi} \tag{2.7}$$

When the integrations are done, this yields the equation for S_b:

$$S_b = \delta\cos\theta\,\frac{\left[\arctan\left(\frac{R+\delta}{R-\delta}\tan\frac{\phi}{2}\right) + \arctan\left(\frac{R-\delta}{R+\delta}\tan\frac{\phi}{2}\right)\right]_{-\Delta\phi-\theta}^{\Delta\phi-\theta}}{\left[\arctan\left(\frac{R+\delta}{R-\delta}\tan\frac{\phi}{2}\right) - \arctan\left(\frac{R-\delta}{R+\delta}\tan\frac{\phi}{2}\right)\right]_{-\Delta\phi-\theta}^{\Delta\phi-\theta}} \tag{2.8}$$

(The equation for S_b for y displacement is the same provided θ is redefined as the angle from the y axis, which is consistent with rotational symmetry, or $\cos\theta$ is

replaced by $\sin\theta$.) When $\Delta\phi$ goes to 0, this gives the derivative of the integral and therefore gives (2.6). When $\delta\cos\theta$ goes to zero

$$\lim_{\delta\to 0} S_b = \frac{R}{2}\frac{\Delta\phi}{\sin\Delta\phi} \tag{2.9}$$

In the limits where $\delta\cos\theta$ and $\Delta\phi$ go to zero, this yields $\frac{R}{2}$.

2.4. Effects of Large Rod Diameter

Most of the BPMs in the SLC were calibrated before installation in order to determine the offsets of their electrical centers from their mechanical centers. The electrical center is defined as the position where the normalized voltage difference is zero; therefore all positions are measured with respect to the electrical center. Calibrations were done by sending a 1 nanosecond wide pulse down a rod passed through the BPM. Generally, these rods were scaled to the BPM diameter in order to give a 50 Ω impedance for the calibration pulse. This impedance matching gives a large pulse on the rod and therefore large signals on the BPM electrodes.

Because the rod is a conductor with a finite diameter, when it is displaced towards one side of the BPM the charge redistributes on the rod and gives a charge movement larger than the physical displacement of the rod. This larger movement of charge gives a larger normalized voltage difference, so the factor S_r that gives the physical displacement of the rod will be smaller than S_b, which gives the physical displacement of a line of charge. Calibration depends on the position of the calibration rod relative to the BPM, so S_r must be calculated and used.

The method used to calculate the effect of finite rod diameter follows from the fact that the equipotentials due to two parallel lines of opposite charge are two sets of cylinders of decreasing radii whose axes converge on the lines of charge (Fig. 4)[2]. The relation between the radii r and positions x of these cylinders is:

$$x^2 - r^2 = a^2 \tag{2.10}$$

where a is half the distance between the two lines of charge and x is the distance from the midpoint between the two lines of charge to the axis of the cylinder.

Now in the case of a calibration rod displaced in a BPM, we have two non-concentric parallel cylindrical equipotentials. Therefore, the problem can be solved by working backwards from the solution for the equipotentials of two parallel and opposite line charges.

Using (2.10), the cylinder whose radius is the BPM radius will give the value of x for the center of the BPM, and the cylinder whose radius is that of the rod will give the value of x for the center of the rod. The difference of these two x values divided by the charge displacement from the center of the BPM will give the correction factor to the previously calculated S_δ, which gives the position of the apparent line of charge from the signals induced on the electrodes of the BPM (2.3).

The displacement of the effective line of charge from the center of the BPM is δ, and its image is at $D = \frac{R^2}{\delta}$ (Fig. 3). Therefore the distance between the two lines of charge is $D - \delta$. X is defined as the distance of the center of an equipotential cylinder to the midline between the lines of charge; therefore

$$X_{BPM} = \frac{D - \delta}{2} + \delta = \frac{D + \delta}{2}$$

R_{BPM} and R_{ROD} are also known. Define the rod displacement (Fig. 5)

$$\sigma = X_{BPM} - X_{ROD}.$$

Using (2.10), we have

$$(\frac{R_{BPM}^2 + \delta^2}{2\delta})^2 - R_{BPM}^2 = (\frac{R_{BPM}^2 + \delta^2}{2\delta} - \sigma)^2 - R_{ROD}^2$$

Solving for δ, dividing by σ, and inverting, we find that the ratio of rod displacement to apparent charge displacement is

$$\frac{\sigma}{\delta} = \frac{2\sigma^2}{(\sigma^2 - R_{ROD}^2 + R_{BPM}^2) - \sqrt{(\sigma^2 - R_{ROD}^2 + R_{BPM}^2)^2 - 4\sigma^2 R_{BPM}^2}} \qquad (2.11)$$

This reduces to 1 in the limit where R_{ROD} goes to zero and to

$$\frac{\sigma}{\delta} = 1 - \frac{R_{ROD}^2}{R_{BPM}^2} \qquad (2.12)$$

when σ goes to 0.

The apparent charge displacement can be calculated from the normalized voltage difference using S_δ; multiplying this by the ratio of displacements (2.12) will give S_r.

3. MEASUREMENT METHODS

3.1. Mechanical Apparatus

All conversion factors were measured in a coordinate system where the electrodes were at 45° to the coordinate axes; this was forced by the geometry of the BPMs, because electrodes were generally at 45° to flat surfaces which were used to position and clamp the BPMs.

Therefore, a slightly different scheme of position calculation employing the difference between all four electrodes was used:

$$x = S_b' \frac{(V_1 + V_4) - (V_2 + V_3)}{V_1 + V_2 + V_3 + V_4} \tag{3.1}$$

$$y = S_b' \frac{(V_1 + V_2) - (V_3 + V_4)}{V_1 + V_2 + V_3 + V_4} \tag{3.2}$$

The conversion factors for these formula can be calculated by the same methods previously used. For small width electrodes, these give $S_b' = \sqrt{2} S_b$.

Apparatus for Measurement of S_r for Arc BPM

To measure S_r for the Arc BPMs, their calibration stand was used. Since the Arc BPMs have a square outer casing, they are clamped in place against two machined surfaces which are at right angles to each other, and the calibration rod slides into the BPM. The calibration rod position can not be changed. The calibration rod will not transfer to another system, so precise movement of the BPM was accomplished by stacking 5 and 10 mil shims, measured by a micrometer, between the BPM and the lower machined surface. The clamp ensured that the BPM sat squarely on the stack of shims. The electronics used to read out the signals on the BPM electrodes were the same for all measurements and will be described later.

Apparatus for S_r Measurement for Final Focus BPM Measurements of S_r for the Final Focus BPM and S_b for both the Arc and Final Focus BPMs were done using three movable stages on a Teflon-coated V-block (Fig. 6). These usually held the calibration apparatus. The center stage was low and supported the plate and clamp used to hold the BPM in place. It had a screw drive to move the plate horizontally at right angles to the V block. This screw was calibrated in mils of movement over a range of about an inch, but it suffered from severe hysteresis. The two stages on

either side of it held vertical plates containing holes into which the calibration rod adapters were fastened. These adapters held the rod in place by means of Teflon washers. These endplates were adjustable in height by means of calibrated screws similar to the one used for horizontal displacements on the center stage.

To measure S_r for Final Focus BPMs, a 2" BPM and its calibration rod was used. The adapter was chosen to hold the rod steady but not make ground contact with the BPM in order to isolate movement of the BPM. The lack of ground contact did not cause much reflection in the fake beam signal because the gaps between the BPM and adapter were much smaller than the length of the pulse, which was 1 nsec. Since the screw which moved the center stage horizontally was not reliable as a measurement of how far it had travelled, a dial gauge micrometer clamped to the table and touching a flat surface of the BPM measured displacement.

Apparatus for Measurement of S_b for Both BPMs

Measurements of S_b were made by the same method described for S_r for the Final Focus BPM, except that all measurements of S_b were made by simulating the beam with a thin wire .345 mm in diameter. This wire was strung through the BPMs clamped onto the center stage of the calibration stand. At each end it was soldered to an SMA bulkhead connector which was fixed to the upright plate. These plates were adjusted in height until the wire was parallel to and well centered in each BPM. The impedance of a wire of that diameter with the BPMs was nearly that of a wire in empty space, so a 330 Ω termination was put on the end of the wire to reduce ringing of the fake beam signal. The 1 nsec wide fake beam pulse was the same as that used for calibration. It was generated and carried to the wire at 50 Ω, so much of it was lost through reflections at the beginning of the wire, but no efficient transformer for a 1 nsec wide pulse was available. Even with the reflection losses, signal levels were high enough for processing.

3.2. Read-out Processing

Signals from the electrodes were processed by electronics controlled through a GPIB interface bus by an IBM PC. The cables went to a programmable relay switch (the HP59306A Relay Actuator) and were switched one at a time into the processor by the computer. The processor, the SLAC-made BPM Calibration System, consisted of a filter and integrator with adjustable attenuators and a trigger which was referenced to the start of the calibration pulse, generated within the same module. The trigger was fixed for each BPM so that the starting time for the integrator coincided with the first negative extremum of the signal from the electrode. For all measurements but the rod in the Arc BPM, the attenuators were

adjusted to give signals between one and two volts per electrode, since digitization error and non-linearities were low in this range. For the rod in the Arc BPM, signals were about .5 V. From the integrator, the signal was sent to a HP3455A programmable digital volt meter which was read out via GPIB by the computer.

The relay switched through each of the four electrodes and was then left open, at which time a fifth reading was taken in order to determine the pedestal, since it slowly varied. This pedestal was subtracted from the signals. This pedestal reading and subtraction was not done for the measurements with the rod in the Arc BPM.

At each position of the rod or wire within the BPM, the series of readings was taken four times. The computer calculated

$$\frac{(V_1 + V_4) - (V_2 + V_3)}{V_1 + V_2 + V_3 + V_4},$$

corresponding to x position, and

$$\frac{(V_1 + V_2) - (V_3 + V_4)}{V_1 + V_2 + V_3 + V_4},$$

corresponding to y position, for each set of readings and for the average of the four sets. The spread within the four x and y positions calculated at a given rod position were used to evaluate the measurement error.

Occasionally, this error was unusually large. The measurement was then repeated without disturbing the position of the BPM with respect to the rod or wire. These measurements were then combined to reduce the error. Large errors could occur for several reasons: movement near the cables affected the pedestals for the electronics, and movement caused vibration in the wire which affected the repeatability of the readings. As time passed, the tension on the wire lessened, increasing the frequency of large errors and necessitating a retightening of the wire between sets of scans. All voltages and calculated quantities were printed out and displayed on the computer screen, so immediate decisions could be made to repeat a measurement. Repeated measurements were averaged.

3.3. Measurement of Response to Displacement

All S were measured by stepping the BPM position through a known set of displacements, calculating the ratio of voltage differences with respect to sums, and fitting the slope of the line relating known displacement to this ratio. This slope is the measured S. The BPM was moved rather than the rod or wire because movement of the rod or wire would have required precise stepping of the supports on both ends and thus would have introduced more error.

To start a scan, the BPM position was adjusted so that all four electrodes read approximately the same signal; this put the scan near the center of the BPM, where the response to position change is nearly linear and which is the region of concern for beam measurements. The dial gauge micrometer used to precisely determine position had a range of 60 mils; therefore most scans were done from 1 to 59 mils in order to stay within that range. The scans were done in steps of four or five mils, so that each scan contained thirteen points and step size was substantially larger than measurement error.

Sets of scans were done from several starting positions in the BPM in order to compensate for possible non-linearities at any one position. Also, some scans were done over a much broader range of distances in order to test non-linearity of S_b. This was done by scanning to the limit of the micrometer, then leaving the BPM fixed while the micrometer was repositioned to the beginning of its range, and then continuing the scan of the BPM. This was repeated until the wire was displaced to about half of the radius of the BPM.

3.4. Analysis of Data

The data were partially analyzed by the computer that made the measurements, since it calculated the normalized voltage differences. These normalized voltage differences and the measured displacements of the BPM were fit to a line by a least squares method. S was defined as the slope m of the line $y = mx + b$, with y the measured displacement and x the normalized voltage difference. Since S was measured in the 45° rotated coordinate system, a factor of $\sqrt{2}$ was removed to get S for a non-rotated coordinate system for the Final Focus BPMs. The Arc BPMs were left in the rotated coordinate system. Although both types are installed in the SLC at 45° to the beam coordinates, these were treated differently because signal processing is done in the rotated frame for the Final Focus BPMs but in the beam coordinates for the Arc BPMs.

There were two basic sources of measurement error: errors in the measurement

of the normalized voltage difference, and position errors resulting from inaccuracies in reading the dial gauge micrometer and positioning the BPM. Errors in the measurement of the normalized voltage difference resulted from digitization errors for the voltage measurements and from vibrations of the wire, which caused small shifts in its position from measurement to measurement. These can be estimated from the rms spread between the four measurements taken at each position of the BPM. The size of these errors varied with the type of scan. For the wire in the Final Focus BPM, its average value was $1.6 \cdot 10^{-4}$, corresponding to a measured position error of 2.9μ. It sometimes grew to 10^{-3} (measured position error 18μ) but retightening the wire at the conclusion of a scan brought it back down, indicating that wire vibrations contributed to this error. For the rod in the Final Focus BPM, this error was $0.6 \cdot 10^{-4}$, or 0.9μ. This is lower than for the wire because the rod is more rigid than the wire. For the wire in the Arc BPM, the signal size was smaller (about 1 volt) so the proportional digitization error was larger, giving a typical rms spread of $2.4 \cdot 10^{-4}$, which corresponds to an error of 1.8μ in measured position. For the rod in the Arc BPM, this error was $1.6 \cdot 10^{-3}$, or 10.2μ in measured position. This comparatively large size reflects the small voltage per electrode (0.5 V) and the drifting of the pedestal, since compensation for the drifting of the pedestal was not made in these scans.

For the measurement of S_r for the Arc BPM, position error was caused in part by shifts in the micrometer measurements of the stack of shims. These were small, about 1μ. The dominant contribution to position error was the fact that the gaps between the shims in the stack could change each time the BPM was clamped on top of the stack. This error accounted for about 1 mil, or 25.4μ.

For the scans done on the moveable stage, errors in the measured position of the BPM resulted from inaccuracies in reading the dial gauge micrometer and shifts in the position of the BPM and the dial gauge micrometer which were not accounted for. The dial gauge micrometer was marked in intervals of 0.5 mils, which leads to an error in reading the relative change in position of about half the marker increment, or 6μ. The tables following in the results section show the calculated start and endpoint of each scan. Those for repeat scans over the same range are consistent with this position error.

Another source of position error is changes in the BPM position which were not recorded. These could occur if the micrometer shifted during repositioning of the BPM, or if the BPM shifted position while the reading was being taken. A similar error could result in the long scans if the BPM shifted during repositioning of the micrometer. All of these errors would show as a discontinuity in the normalized voltage difference *vs.* position curves, but could not be corrected. No obvious error

of this sort appeared. A further error could enter if the number of steps taken were miscalculated; the long scans were particularly prone to this type of error. This error also appears as a discontinuity in the curves, but as it is quantized with respect to step size it is easily recognized and corrected.

Correlation between x and y movement can also induce error. A comparison of the starting and ending points of the scans, shown in the tables in the following section, show a slight correlation, but it is very small: about 3μ movement in y for 1.48 mm movement in x. The long scans show a larger movement in y, but this is in large part due to the fact that S_b changes at large displacement and these starting and ending positions were calculated using a linear approximation to S_b.

Systematic errors can result from a faulty calibration of the dial gauge micrometer, so that it measures the wrong value of distance traveled. This would affect all calculations of S in the same manner. An estimate of accuracy as one increment in the full range gives an error in position of 1%, which translates to an error in S of 1%. Another source of systematic error is a constant pedestal offset in the digitization, which would result in the wrong normalization for the voltage difference. A unaccounted pedestal of 0.01 V would likewise give an error in S of 1%, for a signal size of 1 V per electrode. The last source of systematic error results from the fact that normalized voltage difference is not linear with displacement, whereas S was calculated as the fit to a line. Therefore the value of S depends on the displacement from the center, and the further from the center the scan is done, the larger S will be. This effect was partially corrected by trying to center scans on the center of the BPM and by taking scans over several ranges and averaging the results.

The total estimated error in S is about 1.4% systematic error for all measurements. For measurement fluctuations, the estimated error in S_b for the Arc BPM is 0.028 mm. For S_r for the Arc BPM, it is 0.124 mm. For the Final Focus BPM, $\sigma_{S_b} = 0.071$ mm, and $\sigma_{S_r} = 0.053$ mm.

4. RESULTS

4.1. Final Focus BPM

For the 2″ Final Focus BPM and its calibration rod, a total of nine scans were made over two ranges. Table 2 lists the results of these scans. They are in good agreement, and the average S_r measured was 10.444 ± .017 mm; the quoted r.m.s. deviation is well within the measurement error. Graphs of displacement versus voltage for these scans are shown in Fig. 7. Aside from a change of scale, these graphs are typical for all short range scans.

Table 2

Results of Rod Scans in Final Focus BPMs

Scan	S_r (mm)	Start X (mm)	Start Y (mm)	End X (mm)	End Y (mm)
1	10.446	-0.827	0.033	0.642	0.033
2	10.440	-0.831	0.034	0.643	0.034
3	10.468	-0.833	0.027	0.633	0.033
4	10.448	-0.841	0.034	0.629	0.033
5	10.406	-0.841	0.035	0.633	0.031
6	10.449	-0.841	0.034	0.631	0.031
7	10.425	-0.843	0.031	0.631	0.031
8	10.459	-1.789	0.264	-0.321	0.257
9	10.454	-1.789	0.263	-0.318	0.259

For the wire in the Final Focus BPM, a total of eight scans were made from three starting positions. One scan was extended over a range of 540 mils, more than half of the radius of the BPM (Fig. 8). Table 3 shows the results of individual measurements. The average S_b in the center of the BPM was 12.679 ± .048 mm.

In the 2″ Final Focus BPM, two scans were done with a smaller (15.389 mm diameter) calibration rod in order to further test the effect of rod radius on conversion factor. These scans are shown in Table 4. They gave an average S_r of 11.383 ± .003 mm.

Table 3

Results of Wire Scans in Final Focus BPM

Scan	S_b (mm)	Start X (mm)	Start Y (mm)	End X (mm)	End Y (mm)
1	12.656	-0.772	-0.004	0.697	-0.008
2	12.665	-0.665	0.022	0.817	0.016
3	12.702	-0.645	0.023	0.822	0.020
4	12.717	-0.643	0.025	0.827	0.020
5	12.763	-0.641	0.025	12.288	-0.086
6	12.593	-0.682	0.262	0.792	0.269
7	12.648	-0.674	0.274	0.802	0.279
8	12.687	-0.669	0.280	0.802	0.282

Table 4

Results for Small Rod in Final Focus BPM

Scan	S_r (mm)	Start X (mm)	Start Y (mm)	End X (mm)	End Y (mm)
1	11.386	-0.822	0.027	0.652	0.024
2	11.380	-0.822	0.027	0.648	0.024

4.2. ARC BPM

For the calibration rod in the Arc BPM, 5 scans were done; the starting position could not be altered owing to the mechanical constraints of the measurement setup. The scans were done in two steps of 5 mils and 3 steps of 10 mils. The results of these scans are shown in Fig. 9. They gave an S_r of $6.406 \pm .062$ mm.

For the thin wire in the Arc BPM, eight scans were done from four starting positions. Two scans were continued over 205 mils. The results of the scans are shown in Table 5. S_b shown for the two long scans was calculated using the first 59 mils of the scan, which were over the same area as the other scans. The results of the long range scans are shown in Fig. 10. Average S_b was $7.462 \pm .028$ mm.

Table 5

Results of Wire Scans in Arc BPM

Scan	S_b (mm)	Start X (mm)	Start Y (mm)	End X (mm)	End Y (mm)
1	7.445	0.104	0.228	1.627	0.266
2	7.411	-0.798	-0.110	0.685	-0.106
3	7.442	-0.722	-0.004	0.748	0.002
4	7.460	-0.727	-0.006	0.744	0.002
5	7.502	-0.729	-0.004	0.730	-0.001
6	7.493	-0.731	-0.005	4.451	0.028
7	7.462	-0.950	-0.193	0.532	-0.184
8	7.481	-0.949	-0.193	4.233	[illegible]3

5. Conclusions

5.1. Wire Scans in the Arc BPM

In order to compare the idealized calculations of S made earlier with the responses of the physical BPM, effective radii were used. The effective radius is defined for a given calculation of S as the radius of the ideal BPM for which that approximation is an exact description. S_b measured at the center of the Arc BPM was $7.462 \pm .028$ mm. An effective radius for the Arc BPM has been calculated for each of the equations for S_b derived previously. The long scans of the wires in the BPM were fit to the non-linear functions to obtain effective radii; for the near-center approximations, the measured S_b value was used. These effective radii can be compared with the physical parameters of the BPMs to see whether the ideal calculations are applicable to the reality. The results are shown in Table 6, with only statistical errors quoted. They are generally consistent with each other.

These values for the effective radius correspond to the vacuum pipe radius of the Arc BPM, perhaps slightly shifted to lie between the outer radius of the electrode (8.33 mm) and the inner radius of the vacuum pipe (10.33 mm). Possible explanations for this effect will be discussed later.

Table 6

Effective Radii Calculated for Arc BPM

Measured With	Fit Used	Effective Radius (mm)	Electrode Width
Wire	linear $S_b = \frac{R}{\sqrt{2}}$	10.551 ± 0.040	0°
Wire	linear (2.9)	10.303 ± 0.039	45°
Wire	non-linear (2.6)	10.329 ± 0.063	0°
		10.335 ± 0.048	0°
Wire	non-linear (2.8)	$10.259 \pm .027$	$46.6 \pm 1.8°$
		10.308 ± 0.006	$45.6 \pm 1.0°$
Rod	large rod	9.29 ± 0.55	n.a.
Actual Radius	-	10.33	45°

5.2. Wire Scans in the Final Focus BPM

S_b measured in the central region of the Final Focus 2″ BPM was $12.679 \pm .048$ mm in the coordinate frame where the electrodes lie on the x and y axes. As in the previous section, effective radii of the BPM were calculated from its measured response. These are shown in Table 7.

These values for effective radius of the Final Focus BPM are slightly less than the inner radius of the BPM vacuum pipe. For both the Arc and Final Focus BPMs, the shift inward of the effective radius is probably due to the presence of the electrodes, which distort the fields from those for a perfect cylinder.

5.3. Effects of Large Rod Diameter

In the Arc BPM, the ratio of S_r for the rod to S_b for the wire was .858; using the equation for the effect of finite rod radius (2.12)for a rod of radius 3.50 mm gives

$$1 - .826 = \frac{R_{ROD}^2}{R_{BPM}^2}$$

which gives an effective BPM radius of $9.29 \pm .55$ mm. This value is substantially less than the effective radii calculated from the wire scans, above, which were all

Table 7

Effective Radii Calculated for Final Focus BPM

Measured With	Fit Used	Effective Radius (mm)	Electrode Width
Wire	linear $\frac{R}{2}$	25.358 ± 0.142	0°
Wire	linear (2.9)	24.698 ± 0.138	45°
Wire	non-linear (2.6)	24.309 ± 0.084	0°
Wire	non-linear (2.8)	24.353 ± 0.256	$41.9 \pm 1.6°$
Large Rod	large rod	23.50 ± 0.72	n.a.
Small Rod	large rod	24.07 ± 0.50	n.a.
Actual Radius	-	25.4	45°

between 10.3 and 10.6 mm. This value for the effective radius lies about halfway between the radius of the beampipe and the outer radius of the electrode, which is 8.33 mm.

In the Final Focus BPMs, for the calibration rod of radius 9.865 mm, S_r was measured as 10.444 mm; this gave a ratio of 0.824. Using the same calculation, the effective radius of the BPM is found to be $23.50 \pm .20$ mm, which is lower than those calculated from the wire and lies between the outer radius of the electrode, 21.77 mm, and the radius of the vacuum pipe, 25.4 mm. This is about the same shift with respect to the two physical radii which was found for the Arc BPM. A measurement of S_r made for a rod of smaller radius, 7.695 mm, in the 2" diameter BPM gave 11.383 mm. The calculation of effective radius gives for this rod a value of $24.07 \pm .50$ mm, which is between that for the large rod and that for the wire, although consistent within error with both.

The reduction of the effective radius with increasing rod diameter is caused by the distortion of the fields by the electrodes. For a rod whose radius is of the same magnitude as the electrode radii, the presence of the electrodes will cause redistribution of charge on the surface of the rod which further displace the center of charge in the rod and thus decrease the S_r for the rod. A decrease in S_r changes the ratio of the conversion factors and looks like a decrease in the effective radius of the BPM. More data points corresponding to different rod radii would be necessary in order to determine these deviations more exactly.

5.4. SUMMARY

For BPMs of the type discussed in this paper, it is possible to calculate a fairly accurate S_b by using the formulas given earlier with R the radius of the BPM vacuum pipe. For work with a small radius line of charge in the center of a BPM, the cylindrical approximation works fairly well; the effective radius for the scans done with a wire were near the radius of the vacuum pipe for both types of BPM. It is only in the case of a large radius conductor carrying the charge that this approximation fails. It probably also fails for very large displacements of a line of charge from the center of the BPM, but within the ranges scanned the non-linear formulas calculated using the cylindrical approximation describe the behavior of the BPM fairly well. Since the ranges scanned covered more than half the distance to the electrodes, this accounts for the region of the BPM which normally is used.

The response of a BPM to a calibration rod is dependent on the electrode configuration and should probably be measured.

The motivation for performing these measurements was to determine S_b and S_r for these BPMs. With the beam approximated by a charge pulse moving along a narrow wire, S_b was calculated to be $12.679 \pm 0.071 \pm 0.178$ mm for the 2" Final Focus BPMs and $7.462 \pm 0.028 \pm 0.104$ mm for the Arc BPMs. S_r was measured as $10.444 \pm 0.053 \pm 0.146$ mm and $6.406 \pm 0.124 \pm 0.090$ mm, respectively.

6. Acknowledgements

I would like to thank Jacques Haissinski, John Sheppard, and Chang Kee Jung for useful discussions on the calculations in this paper.

APPENDIX A: Calculations of S for $\frac{\pi}{4}$ Rotated Electrodes

It is possible to use all four electrodes to calculate the x and y positions of the beam rather than using two for x and two for y. This amounts to a rotation of $-\frac{\pi}{4}$ of the BPM coordinate system. The position equations then become

$$x = S\,\frac{(V_1 + V_4) - (V_2 + V_3)}{(V_1 + V_2) + (V_3 + V_4)}$$

and

$$y = S\,\frac{(V_1 + V_2) - (V_3 + V_4)}{(V_1 + V_2) + (V_3 + V_4)}.$$

Calculating S by the same method as before, the near-center, zero-width approximation is now

$$S = \frac{R}{\sqrt{2}}.$$

The value of S for all displacements, still using zero-width electrodes (the analog to) is

$$S_x = \frac{(R^2 + \delta^2)(R^4 + \delta^4)}{\sqrt{2}R[(R^2 + \delta^2)^2 - 2R^2\delta^2\cos(2\theta)}$$

and

$$S_y = \frac{(R^2 + \delta^2)(R^4 + \delta^4)}{\sqrt{2}R[(R^2 + \delta^2)^2 + 2R^2\delta^2\cos(2\theta)}.$$

For the non-linear S with 2ϕ electrodes, the equations become

$$S_x = \frac{[f(\delta,\phi)]_{a+\frac{\pi}{4}}^{b+\frac{\pi}{4}} + [f(\delta,\phi)]_{a+\frac{7\pi}{4}}^{b+\frac{7\pi}{4}} - [f(\delta,\phi)]_{a+\frac{3\pi}{4}}^{b+\frac{3\pi}{4}} - [f(\delta,\phi)]_{a+\frac{5\pi}{4}}^{b+\frac{5\pi}{4}}}{[f(\delta,\phi)]_{a+\frac{\pi}{4}}^{b+\frac{\pi}{4}} + [f(\delta,\phi)]_{a+\frac{7\pi}{4}}^{b+\frac{7\pi}{4}} + [f(\delta,\phi)]_{a+\frac{3\pi}{4}}^{b+\frac{3\pi}{4}} + [f(\delta,\phi)]_{a+\frac{5\pi}{4}}^{b+\frac{5\pi}{4}}}$$

and

$$S_y = \frac{[f(\delta,\phi)]_{a+\frac{\pi}{4}}^{b+\frac{\pi}{4}} + [f(\delta,\phi)]_{a+\frac{3\pi}{4}}^{b+\frac{3\pi}{4}} - [f(\delta,\phi)]_{a+\frac{5\pi}{4}}^{b+\frac{5\pi}{4}} - [f(\delta,\phi)]_{a+\frac{7\pi}{4}}^{b+\frac{7\pi}{4}}}{[f(\delta,\phi)]_{a+\frac{\pi}{4}}^{b+\frac{\pi}{4}} + [f(\delta,\phi)]_{a+\frac{3\pi}{4}}^{b+\frac{3\pi}{4}} + [f(\delta,\phi)]_{a+\frac{5\pi}{4}}^{b+\frac{5\pi}{4}} + [f(\delta,\phi)]_{a+\frac{7\pi}{4}}^{b+\frac{7\pi}{4}}}$$

where $a = -\Delta\phi - \theta$ and $b = \Delta\phi - \theta$ and

$$f(\delta,\phi) = \arctan\left(\frac{R+\delta}{R-\delta}\tan\frac{\phi}{2}\right)$$

Appendix B: Comparison of S Approximations

In order to demonstrate the errors caused by the use of an approximation to the correct conversion factor, the response of a BPM to motions of the beam has been modelled. The non-linear conversion factor calculated for wide electrodes has been assumed correct for the purpose of these calculations, and response was calculated for a line-like beam and a BPM of two inch radius and electrodes covering $\frac{\pi}{4}$ in ϕ. For a given position of the BPM, this conversion factor was inverted to calculate the normalized voltage difference. Then all of the beam conversion factors were multiplied by this normalized voltage difference to give a "measured" position. The results of these calculations are shown in four sets of two graphs, Figures 11 through 18. The first of each pair shows the results for calculations done in the non-rotated coordinate system, where the electrodes are along the beam coordinate axes, and the second of each pair shows the results for calculations done in the rotated coordinate system, where the electrodes are at $\frac{\pi}{4}$ to the beam coordinate axes.

In all figures, curve *a* is the wide electrode non-linear calculation (assumed correct: note that it is a straight line), curve *b* is the zero-width electrode non-linear calculation, and curve *c* is the linear calculation.

The first figure in each series shows the "measured" x position versus the "actual" x position, given by the wide-electrode non-linear calculation, Fig. 11 for the non-rotated BPM and Fig. 12 for the BPM with electrodes rotated by $\frac{\pi}{4}$.

The second figure in each series shows the "measured" x position versus the "actual" x position, given by the wide-electrode non-linear calculation, for a beam displaced in y by 2 mm. Fig. 13 shows the curves for the non-rotated BPM and Fig. 14 for the BPM with electrodes rotated by $\frac{\pi}{4}$.

The third figure in each series shows the "measured" y position versus the "actual" x position, given by the wide-electrode non-linear calculation, for a beam displaced in y by 2 mm. Fig. 15 shows curves for the non-rotated BPM and Fig. 16 for the BPM with electrodes rotated by $\frac{\pi}{4}$.

The fourth figure in each series shows the "measured" x position versus the "actual" x position, given by the wide-electrode non-linear calculation, for a beam displaced along $x = y$. Fig. 17 shows calculations for the non-rotated BPM and Fig. 18 for the BPM with electrodes rotated by $\frac{\pi}{4}$.

Note that the two non-linear approximations agree fairly well over the whole radius of the BPM, diverging by about 10% in the worst case. The linear approxi-

mation, however, becomes unreliable at about 40% of the BPM radius. For BPMs of smaller radii, the graphs should remain the same except for scaling of the axes. Given the complexity of the wide-electrode calculation, the zero-width electrode calculation would be adequate for most purposes. The linear approximation is only valid in the region near the center of the BPM.

FIGURE CAPTIONS

1) Cross Section of Arc BPM

2) Cross Section of Final Focus 2″ BPM

3) Charge Distribution on a Conducting Cylinder from a Line Charge Displaced from its Axis

4) Equipotentials from Two Parallel Lines of Opposite Charge

5) Conducting Rod Displaced in a Conducting Cylinder

6) Measurement Stand

7) Scans of Final Focus Calibration Rod

8) Long Scan of Wire in Final Focus BPM with Fitted Non-Linearity Curve

9) Scans of ARC Calibration Rod

10) Long Range Scans of Wire in Arc BPM, with Fitted Non-Linearity Curve

11) Measured vs. actual x displacements in a one inch non-rotated BPM: comparison of S_b calculations with ansatz: curve a is the wide-electrode non-linear calculation, assumed correct; curve b is the zero-width-electrode non-linear calculation; and curve c is the linear approximation.

12) Measured vs. actual x displacements in a one inch rotated BPM: comparison of S_b calculations with ansatz: curve a is the wide-electrode non-linear calculation, assumed correct; curve b is the zero-width-electrode non-linear calculation; and curve c is the linear approximation.

13) Measured vs. actual x displacements in a one inch non-rotated BPM with the beam displaced 2 mm in y: curve a is the wide-electrode non-linear calculation, assumed correct; curve b is the zero-width-electrode non-linear calculation; and curve c is the linear approximation.

14) Measured vs. actual x displacements in a one inch rotated BPM with the beam displaced 2 mm in y: curve a is the wide-electrode non-linear calculation, assumed correct; curve b is the zero-width-electrode non-linear calculation; and curve c is the linear approximation.

15) Measured y vs. actual x displacements in a one inch non-rotated BPM with the beam displaced 2 mm in y: curve a is the wide-electrode non-linear calculation, assumed correct; curve b is the zero-width-electrode non-linear

calculation; and curve *c* is the linear approximation.

16) Measured y vs. actual x displacements in a one inch rotated BPM with the beam displaced 2 mm in y: curve *a* is the wide-electrode non-linear calculation, assumed correct; curve *b* is the zero-width-electrode non-linear calculation; and curve *c* is the linear approximation.

17) Measured x vs. actual x displacements in a one inch non-rotated BPM with the beam displaced along $x = y$: curve *a* is the wide-electrode non-linear calculation, assumed correct; curve *b* is the zero-width-electrode non-linear calculation; and curve *c* is the linear approximation.

18) Measured x vs. actual x displacements in a one inch rotated BPM with the beam displaced along $x = y$: curve *a* is the wide-electrode non-linear calculation, assumed correct; curve *b* is the zero-width-electrode non-linear calculation; and curve *c* is the linear approximation.

REFERENCES

1. C. R. Carman and J. L. Pellegrin, SLAC-PUB-1227(1973)
2. W.E. Rogers,**Electric Fields**, McGraw Hill, N.Y., 1954

ARC BPM Croos Section

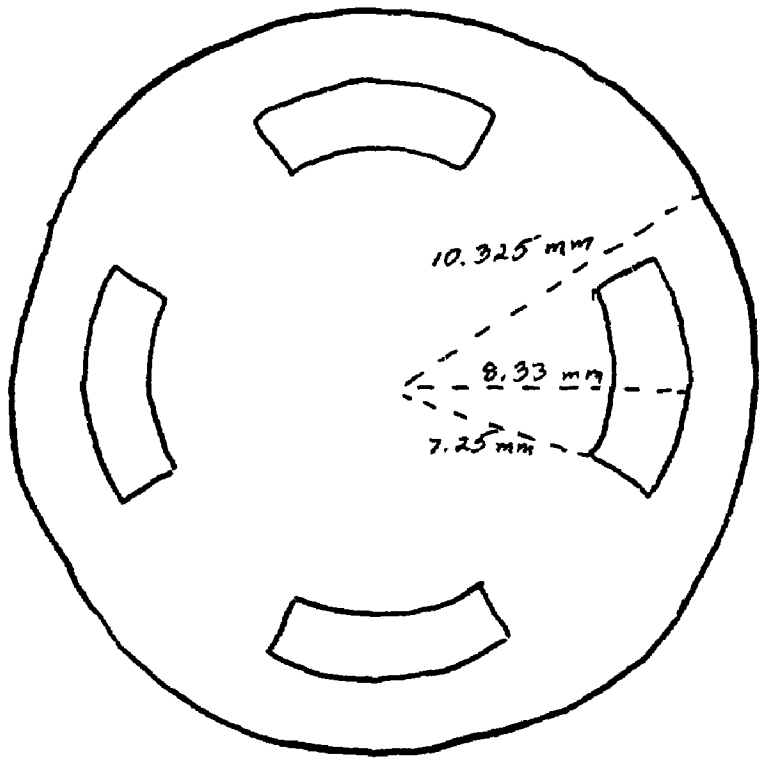

Fig. 1

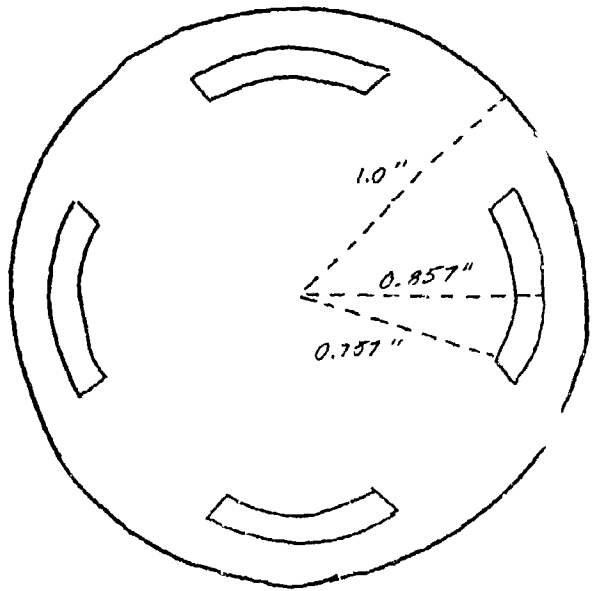

Fig. 2

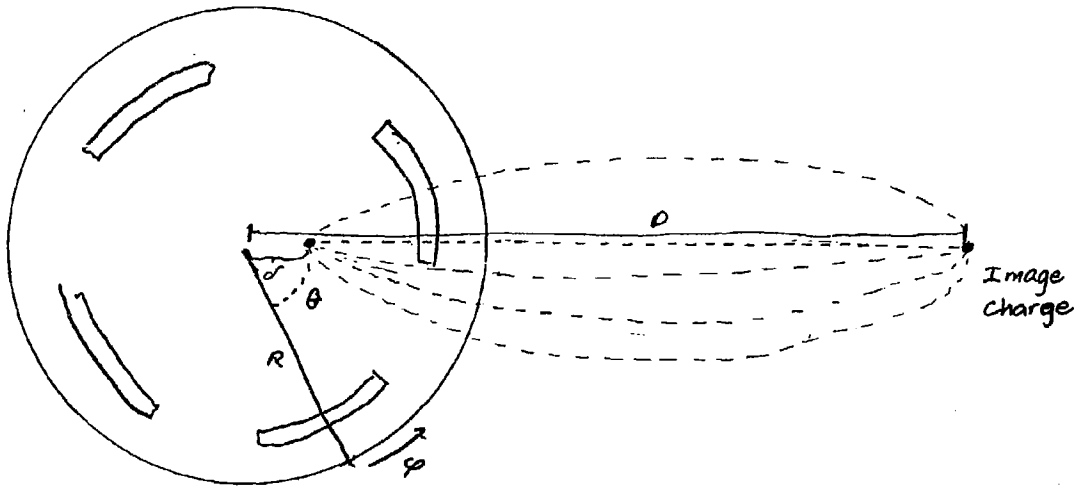

Fig. 3

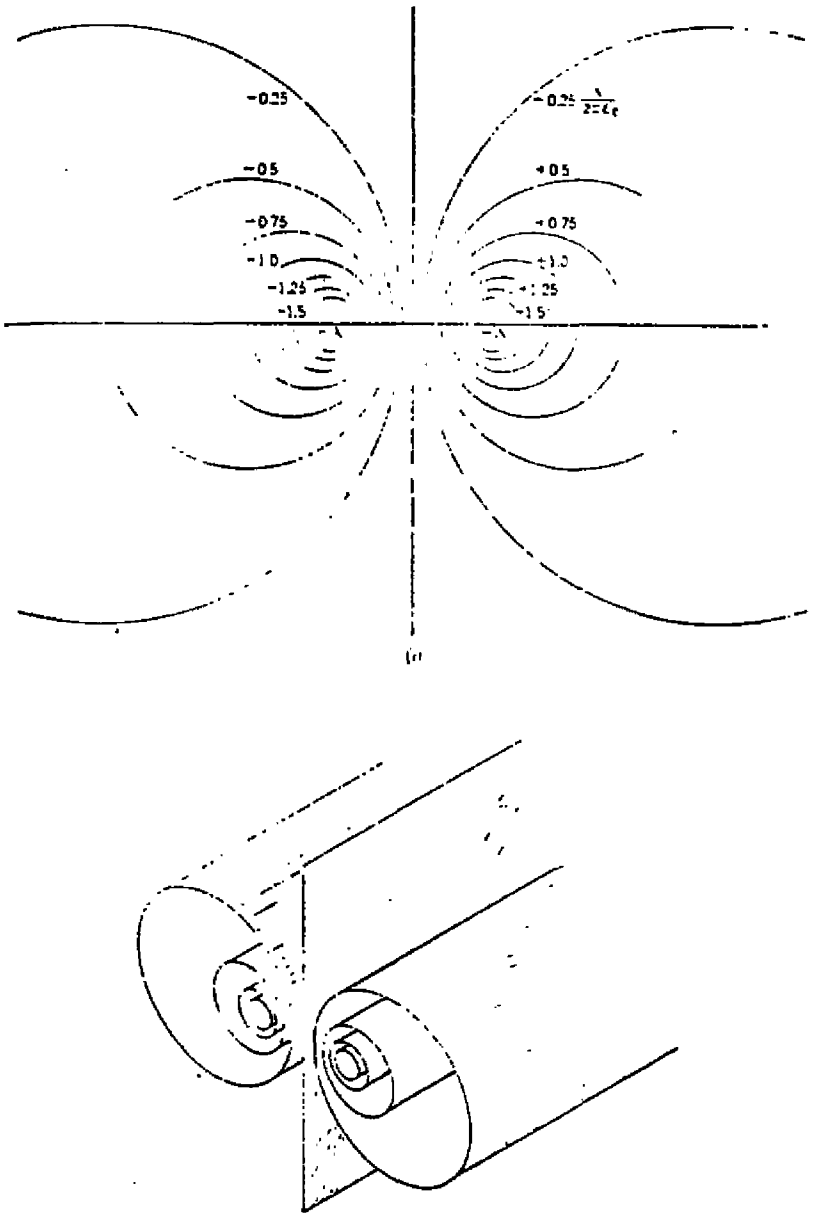

FIG. 3.6 Equipotential cylinders in the field of two line charges, equal, opposite, and infinitely long. In *a* the circles are traces of the equipotential surfaces on a plane perpendicular to the line charges. The three-dimensional character of the cylindrical equipotential surfaces is indicated by *b*.

Fig 4

Fig. 15

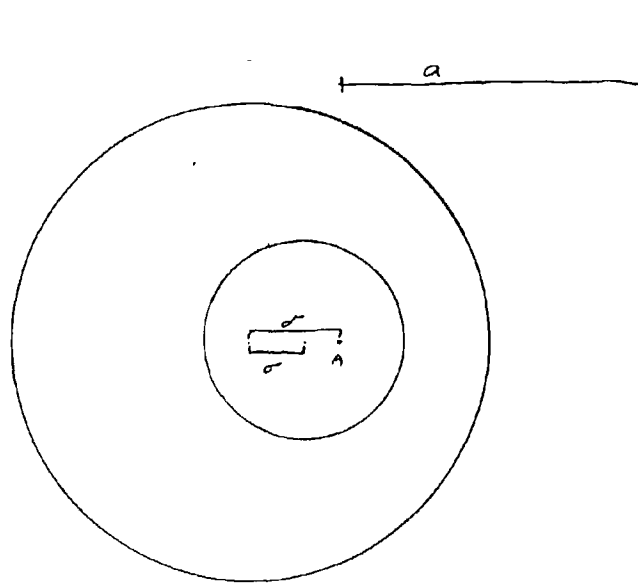

A = apparent position of line of charge

a = distance from A to midline between A and image charge.

δ = displacement of line of charge from BPM center

σ = displacement of rod from BPM center.

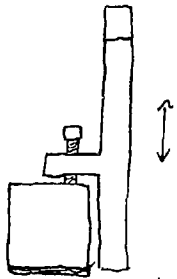

A, side view

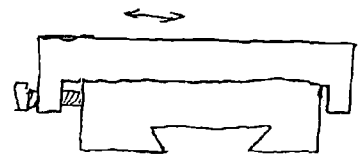

B, front view

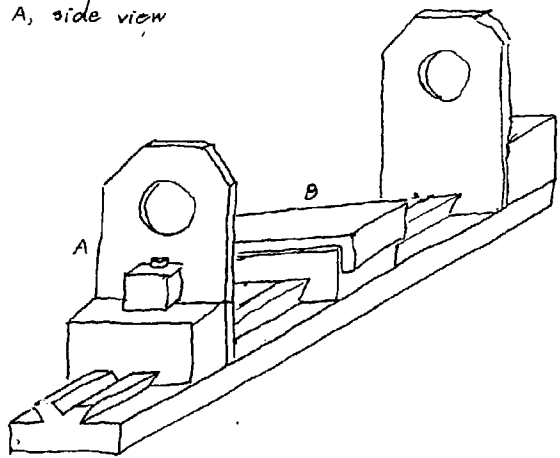

Fig. #6

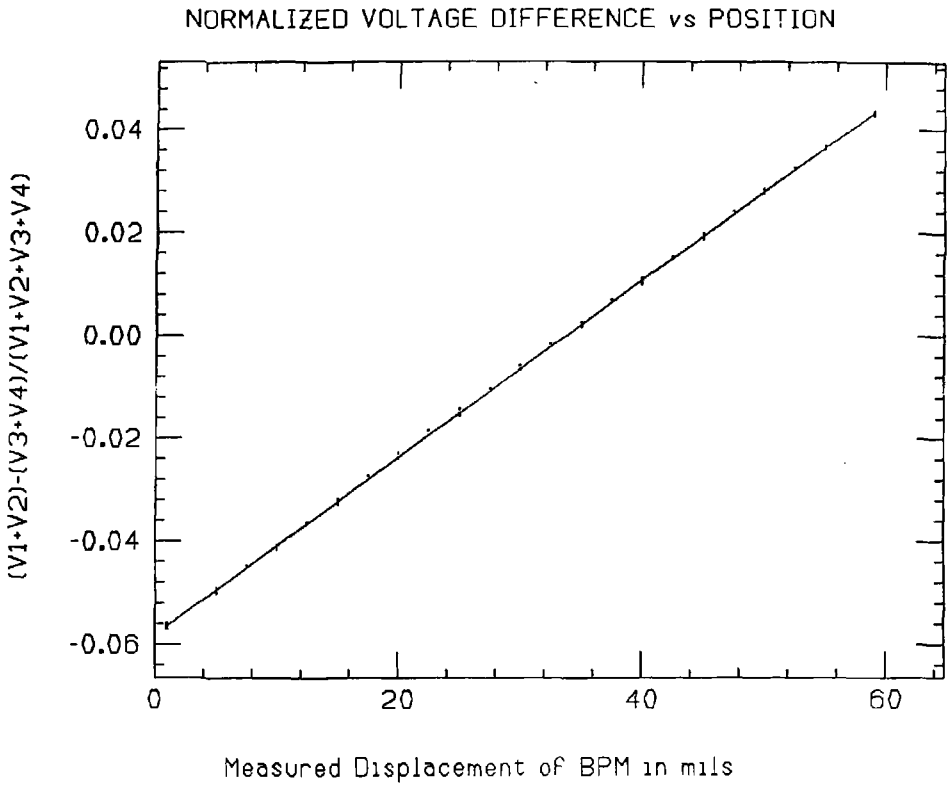
NORMALIZED VOLTAGE DIFFERENCE vs POSITION
(V1+V2)-(V3+V4)/(V1+V2+V3+V4)
0.04
0.02
0.00
-0.02
-0.04
-0.06
0
20
40
60
Measured Displacement of BPM in mils

Fig. 17

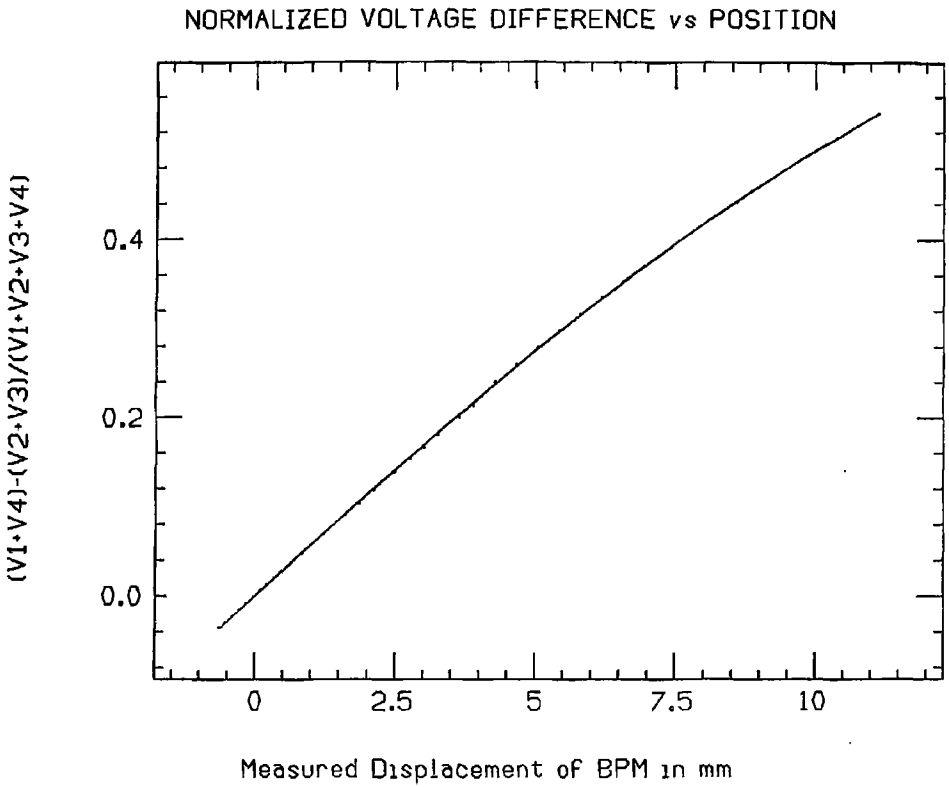
NORMALIZED VOLTAGE DIFFERENCE vs POSITION
(V1+V4)-(V2+V3)/(V1+V2+V3+V4)
0.4
0.2
0.0
0
2.5
5
7.5
10
Measured Displacement of BPM in mm

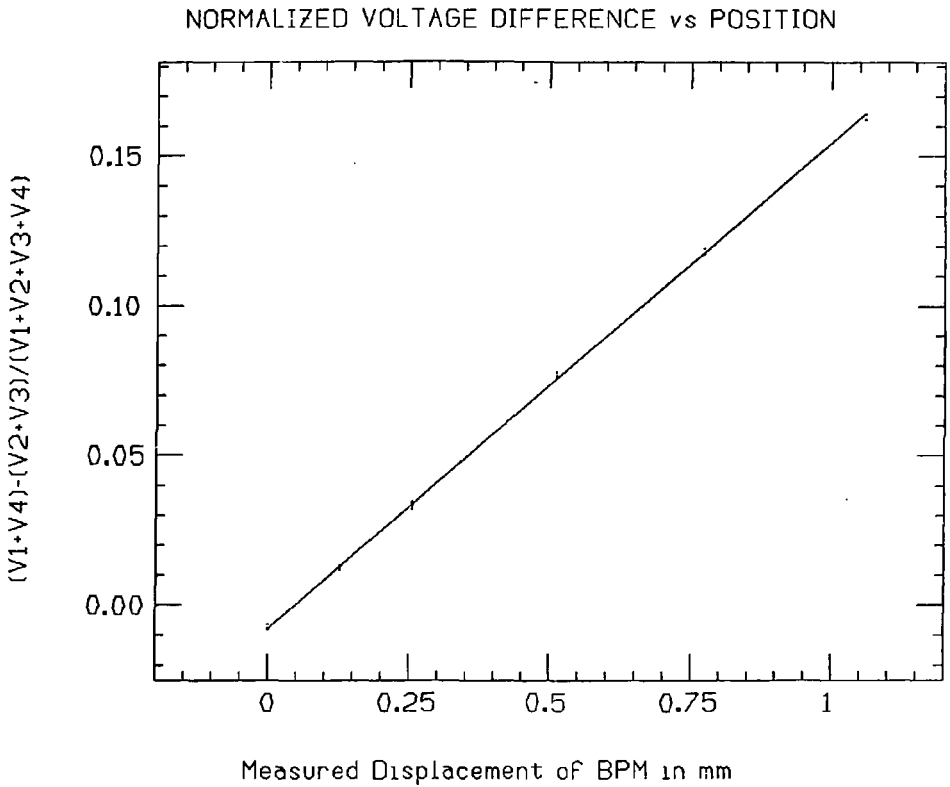
NORMALIZED VOLTAGE DIFFERENCE vs POSITION
(V1+V4)-(V2+V3)/(V1+V2+V3+V4)
0.15
0.10
0.05
0.00
0
0.25
0.5
0.75
1
Measured Displacement of BPM in mm

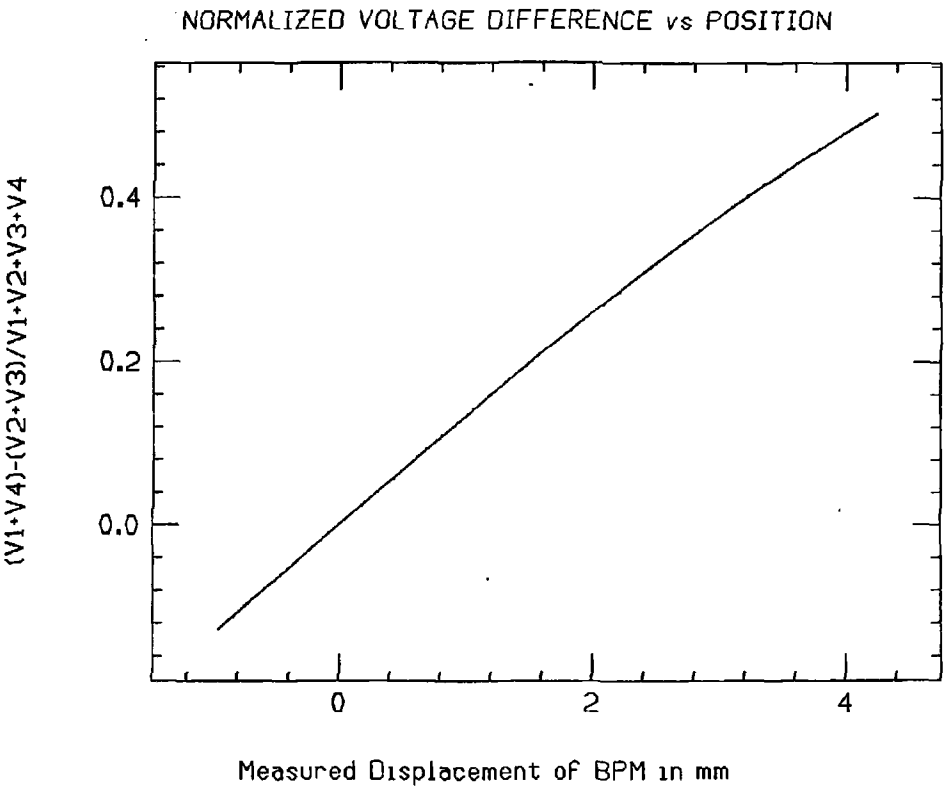

Fig. [redacted]

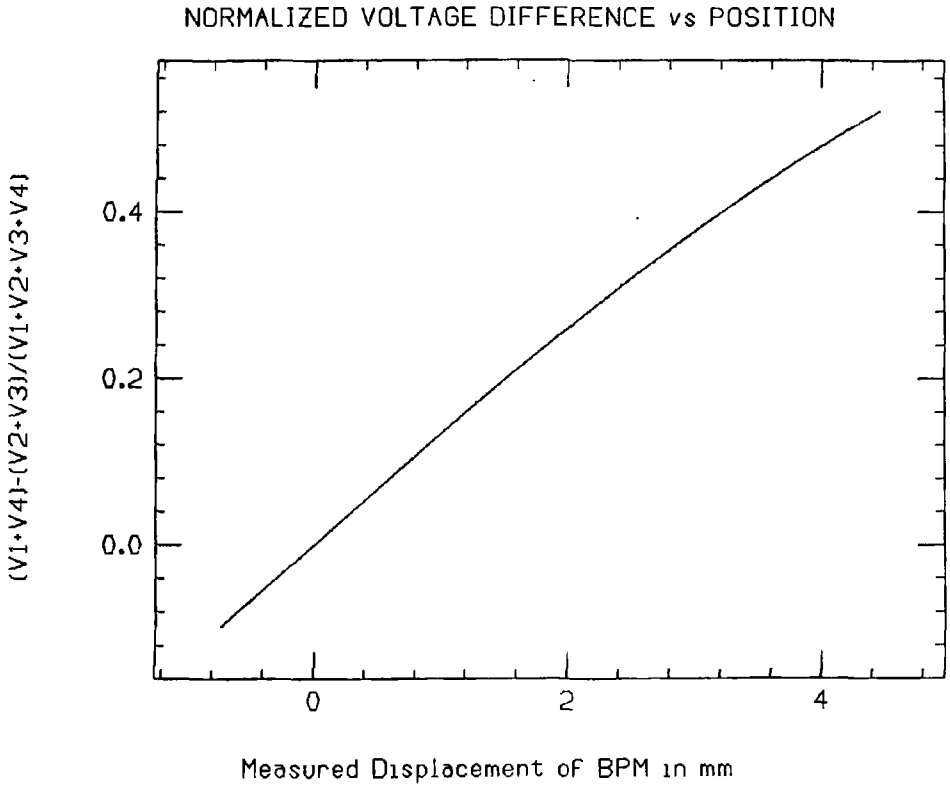

Fig. [redacted] 104

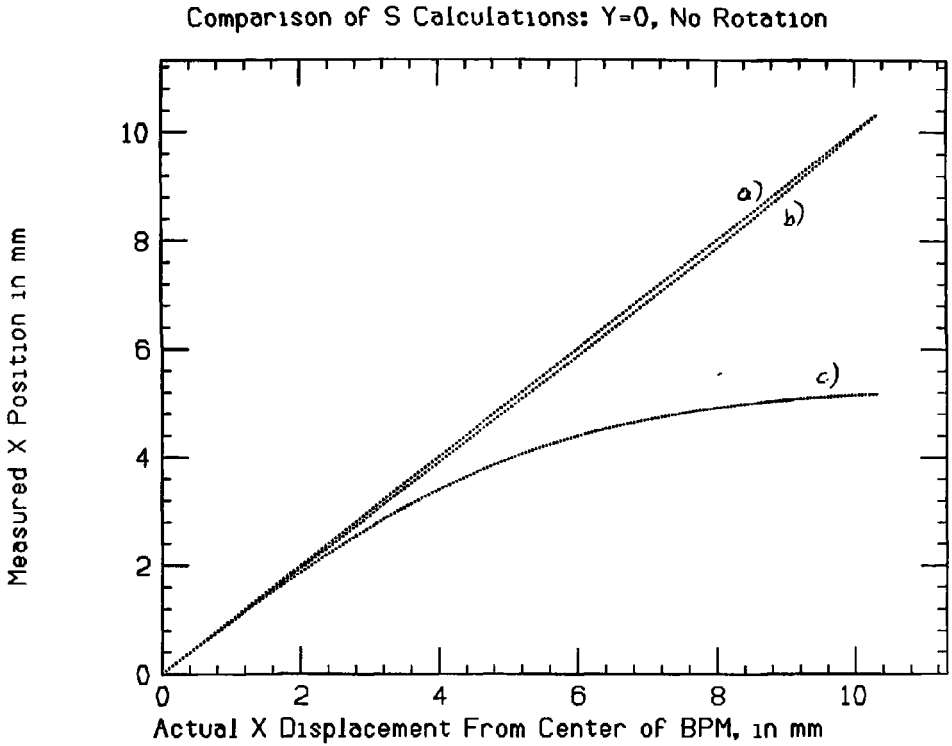
Comparison of S Calculations: Y=0, No Rotation
Measured X Position in mm
Actual X Displacement From Center of BPM, in mm
a)
b)
c)
0
2
4
6
8
10

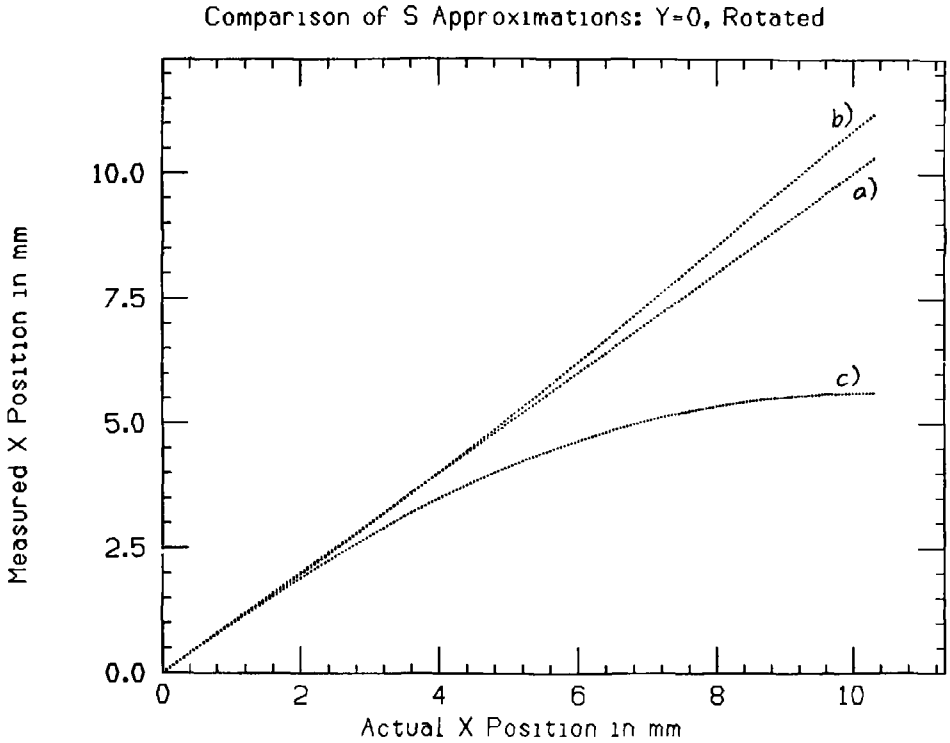
Comparison of S Approximations: Y=0, Rotated
Measured X Position in mm
10.0
7.5
5.0
2.5
0.0
0
2
4
6
8
10
Actual X Position in mm
b)
a)
c)

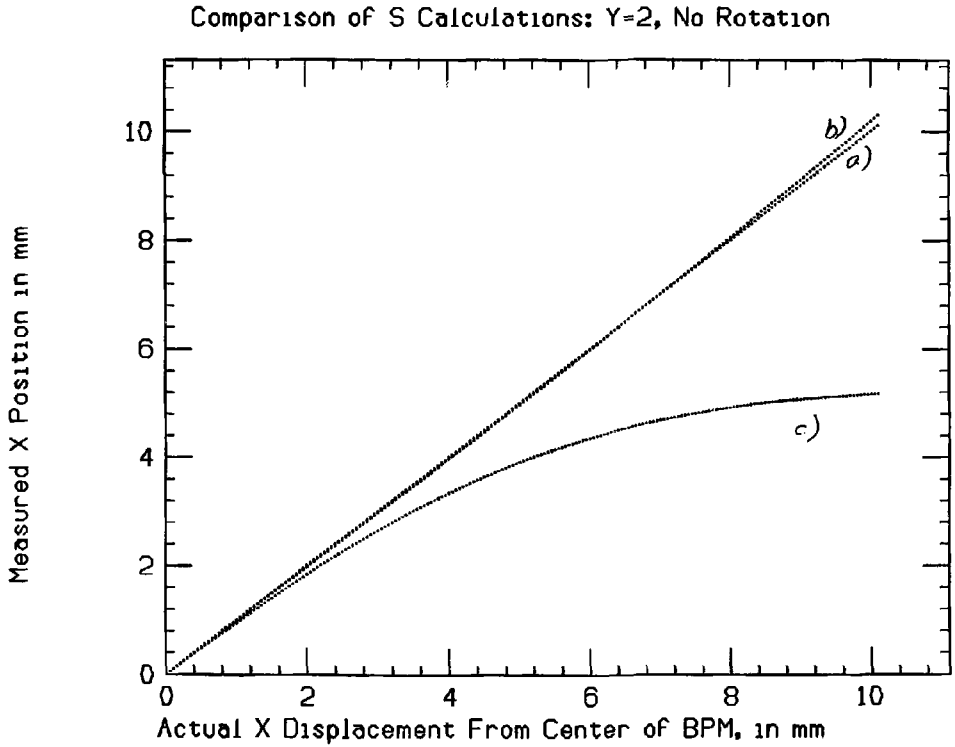
Comparison of S Calculations: Y=2, No Rotation
Measured X Position in mm
Actual X Displacement From Center of BPM, in mm
0
2
4
6
8
10
a)
b)
c)

Fig 13.

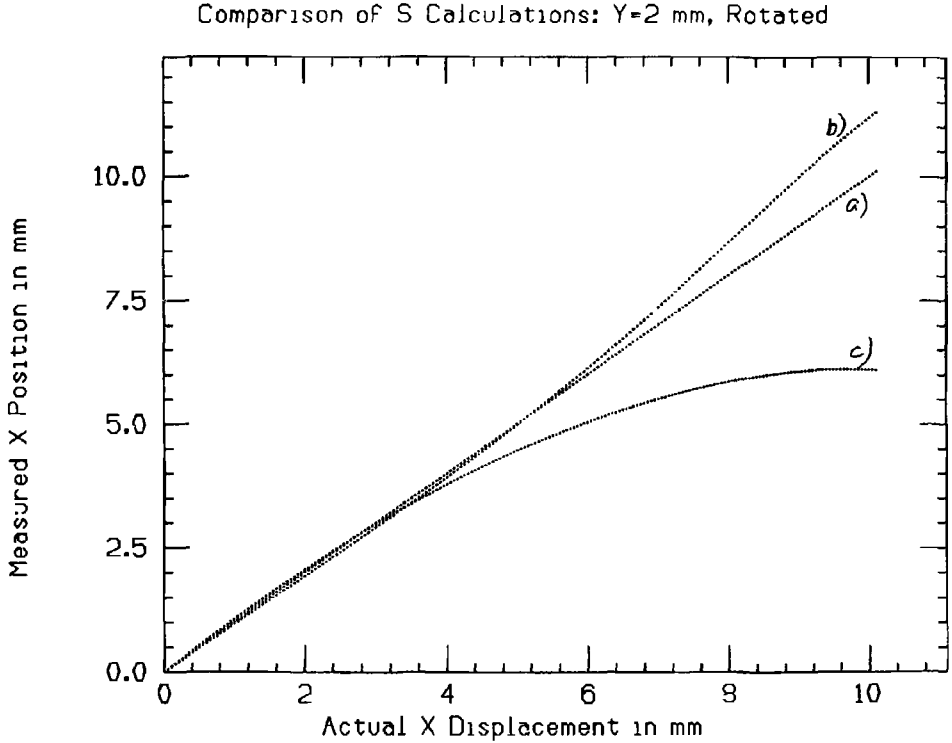
Comparison of S Calculations: Y=2 mm, Rotated
Measured X Position in mm
10.0
7.5
5.0
2.5
0.0
0
2
4
6
8
10
Actual X Displacement in mm
b)
a)
c)

Fig. 10a

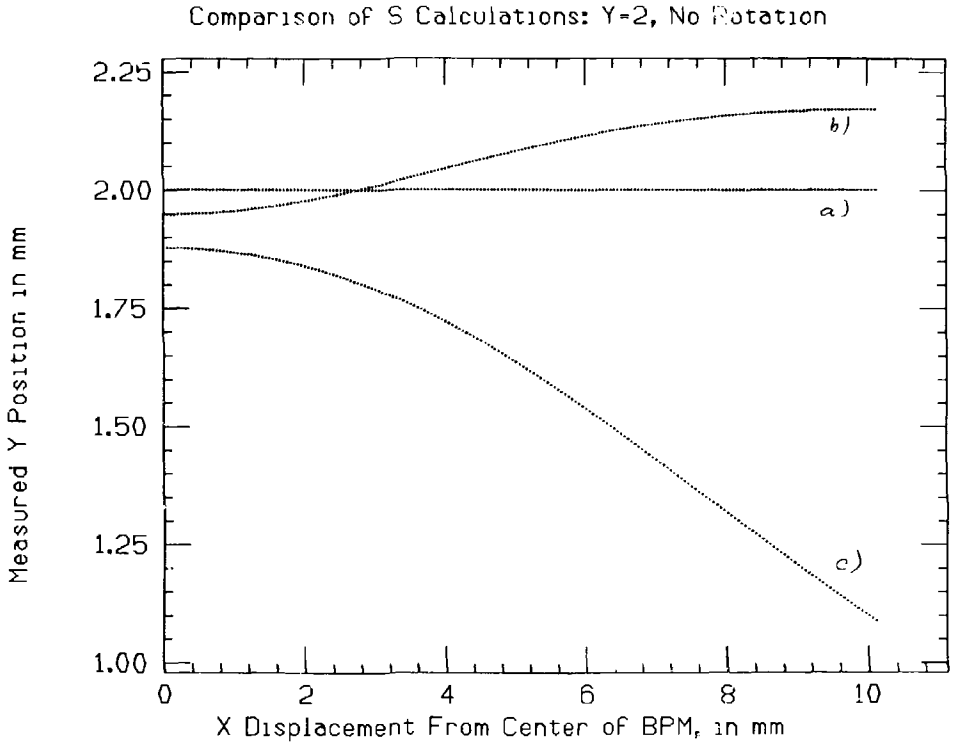
Comparison of S Calculations: Y=2, No Rotation
Measured Y Position in mm
2.25
2.00
1.75
1.50
1.25
1.00
0
2
4
6
8
10
X Displacement From Center of BPM, in mm
b)
a)
c)

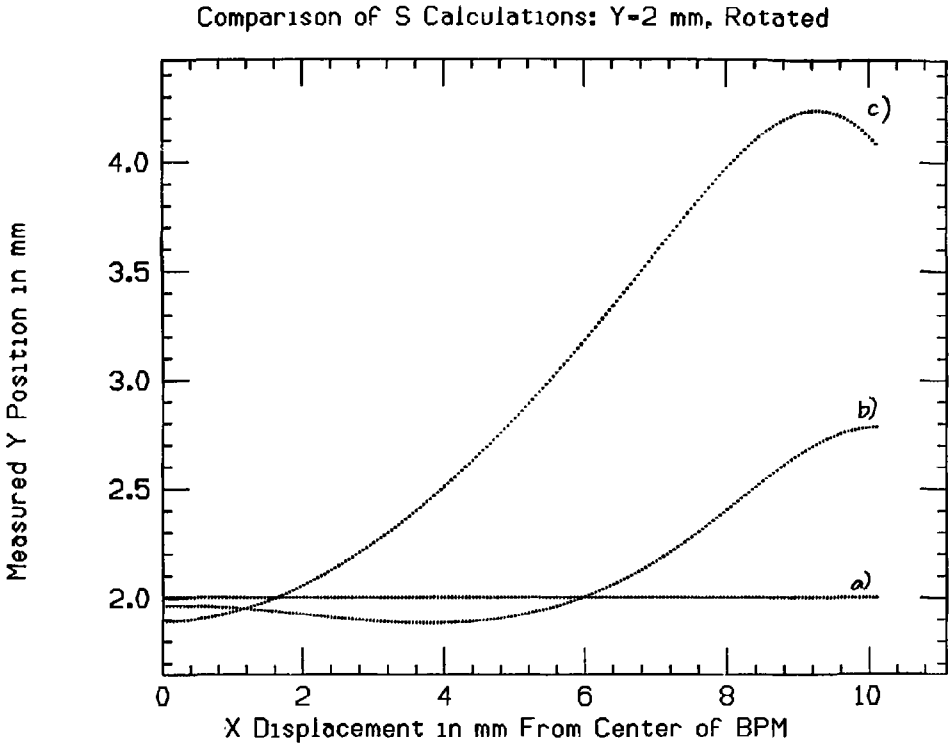
Comparison of S Calculations: Y=2 mm, Rotated
Measured Y Position in mm
4.0
3.5
3.0
2.5
2.0
0
2
4
6
8
10
X Displacement in mm From Center of BPM
c)
b)
a)

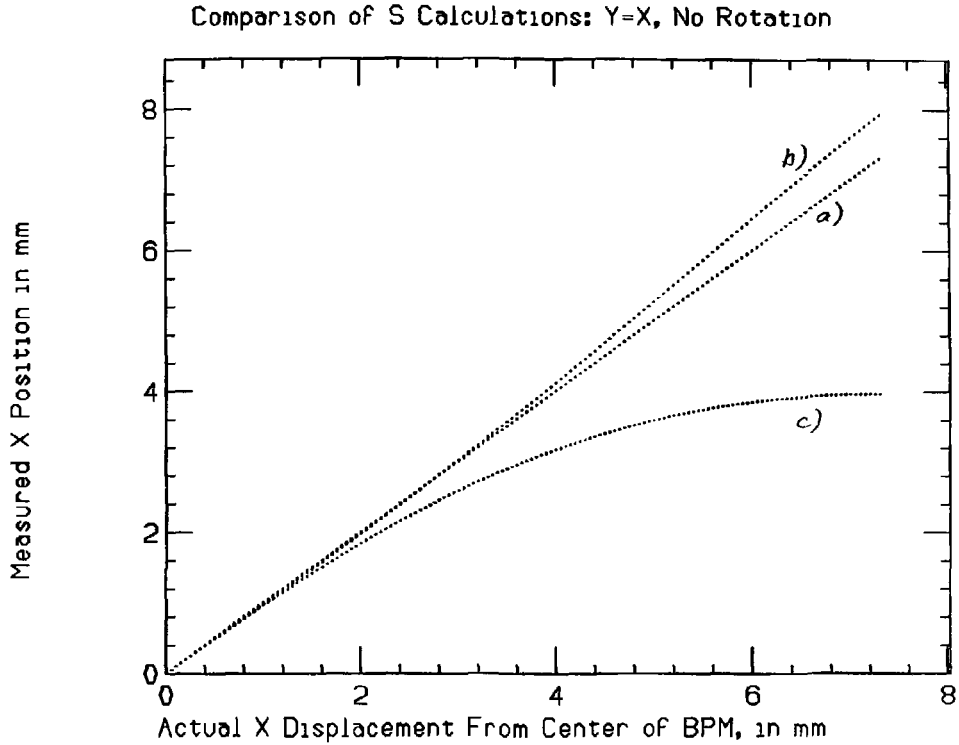
Comparison of S Calculations: Y=X, No Rotation
Measured X Position in mm
Actual X Displacement From Center of BPM, in mm
0
2
4
6
8
a)
b)
c)

Fig

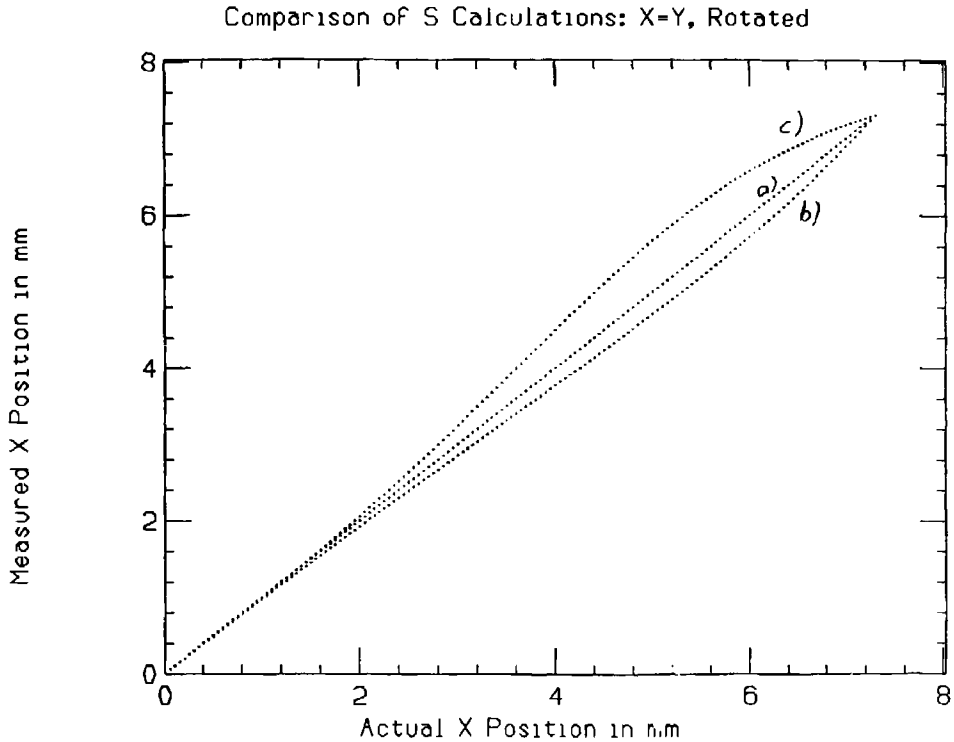
Comparison of S Calculations: X=Y, Rotated
Measured X Position in mm
Actual X Position in mm
0
2
4
6
8
a)
b)
c)